*Pak. J. Bot.*, 47(2): 571-579, 2015.

# SOIL MOISTURE DYNAMICS OF *CARAGANA KORSHINSKII* WOODLAND IN LOESS PLATEAU OF NORTHWEST CHINA

**ZONGXI CHE[1*], XIANDE LIU[1], XUELI ZHANG[2], YE LI[3], ZONGQI CHE[4], MING JIN[1], WENMAO JING[1], XUELONG ZHANG[1], YILIN WANG[1], SHUNLI WANG[1] AND WEIJUN ZHAO[1]**

[1]*Gansu province Qilian water resource conservation forest research institute, Zhangye 734000, China;*
[2]*State Key Laboratory of Grassland and Agro–Ecosystems, School of Life Sciences, Lanzhou University, Lanzhou 730000, China;*
[3]*Zhangye city Ganzhou environmental conservation district, Zhangye, 734000, China*
[4]*Zhangye city environmental conservation district, Zhangye, 734000, China*
[*]*Corresponding author's e-mail: chezongxi@126.com*

**Abstract**

Root water uptake is an important process of water circle and a component of water balance in the field. It should be understood better and effectively. A quantitative method of determining root water uptake should be built for efficient water use. The aims of this paper were to develop a water uptake model for single *Caragana Korshinskii* individual and to validate the model with soil water content in a plantation. Tube–time domain reflectometry (TDR) was used to measure soil volumetric water content, and sap flow sensors based on stem–heat technology were used to monitor locally the sap flow rates in the stems of *C. Korshinskii*. Root density distribution was determined and soil hydraulic characteristics parameters were fitted from measurements. A root water uptake model was established, which includes root density distribution function, potential transpiration and soil water stress–modified factor. The measured data were compared against the outputs of transpiration rate and soil water contents from the numerical simulation of the soil water dynamics that uses Richards' equation for water flow and the established root uptake model. The results showed an excellent agreement between the measured data and the simulated outputs, which indicate that the developed root water uptake model is effective and feasible.

**Key words:** Soil moisture; Root length density; Root water uptake.

## Introduction

Soil moisture is a crucial factor in controlling hydrological and ecological processes. Hydrologically, it plays an important role in generating runoff, consequently, influencing erosion and sediment loads in different temporal and spatial scale (Morgenschweis, 1984; Yang & Tian, 2004; Lacombe *et al*., 2008). Ecologically, it controls vegetation distribution and development (Cheng, 2002; He *et al*., 2003; Chen *et al*., 2007). However, vegetation has an effect on soil moisture by root water uptake, especially in arid and semiarid areas. A lot of literatures reported forest caused a dried soil layer in the profile on Loess Plateau of China due to unbalance between water demand and water supply (Li, 1983; Huang *et al*., 2004; Kimura *et al*., 2007). The dried layer in the soil profile resists forest growth, finally resulting in forest degradation (Li, 2001; Li & Huang, 2008; Wang *et al*., 2008).

The climate in Chinese Loess Plateau belongs to semiarid climate with about 400 mm precipitation falling in the form of rain–storms. The loess material and the characteristic of precipitation cause severe soil erosion and water loss (Meng, 1997). To mediate the soil erosion and water loss in the plateau, the campaign of planting trees and grasses has been conducted since1980s to stabilize the land surface and to retain more precipitation in the soils. There is considerable debate about the selection of afforestation tree species. Generally, the role of species selected depends on cost and effectiveness, that is, when labor and money would devote to planting trees and grasses, the planted species should play a role in preventing from soil and water loss in a long time. When ecological values are aimed, *Caragana Korshinskii* maybe the optimal selection in this area, because it can endure drought by developed root system.

The physiological and ecological characteristics of *C. Korshinskii* have been studied (Xu *et al*., 2006). Some studies reported its role in stabilizing land surface (Donaldson & Lausberg, 1998; Fromm *et al*., 2003). There are a lot of reports about biomass of *C. Korshinskii* and its corresponding environmental factors (Schroth, 1995; Odhiambo *et al*., 1999). However, the relationship between the root distribution of *C. Korshinskii* and soil moisture in Chinese Loess Plateau has been little investigated. So the soil hydrological processes with the development of the species cannot be explained. Therefore some questions cannot be answered, such as, whether the dry layer would appear after the species should be planted, whether it is optimal species to be selected in the semiarid climatic condition. Root water uptake model is a useful tool to understand the relationship between root distribution and soil moisture (Green *et al*., 2003; Lai & Katul, 2003).

In literatures, roots often were classified into fine, small, medium and coarse groups. Among them, the fine roots (diameter < 2 mm) are the most active in the absorption of water and nutrients (Schenk & Jackson, 2002). The distribution of fine roots is an important parameter in root water uptake models (Feddes *et al*., 1976; Feddes *et al*., 1978; Gardner, 1991). Some models only consider the vertical root distribution (Feddes *et al*., 1976; Molz, 1981), some others take account of the vertical and horizontal distribution (Millikin & Bledsoe, 1999; Valverde–Barrantes *et al*., 2007; Macinnis–Ng *et al*., 2010). But these models have mainly been developed for crops, there are few models for shrubs.

Our objectives were: (1) to determine the distribution of fine root of *C. korshinskii*; (2) to determine the relationship between fine root distribution and soil moisture; (3) to build root water uptake model of *C. korshinskii* to estimate soil water content. The results will lay foundation for ecological restoration in Chinese Loess Plateau.

## Materials and Methods

**Study site:** The study was conducted from June to October of 2012 in the Anjiapo catchment, Dingxi County (35°35′N, 104°39′E) of Gansu province in western Chinese Loess Plateau. The annual mean precipitation is 420 mm with great season variations. Over 60% of the precipitation falls between July and September and over 50% occurs in the form of storms. The average monthly air temperature ranges from -7.4 to 27.5°C, with mean annual temperature of 6.3°C. Average annual pan evaporation is 1510 mm. The predominant gray calcareous soil developed on loess parent material with silt texture has a relatively thick profile.

The study area is covered by sparse vegetation, dominated by *Pinus tabuliformis*, *Populus tomentosa*, *Prunus armeniaca*, *Robinia pseudoacacia*, *Caragana korshinskii, Hippophae rhamnoides*. *C. korshinskii* is a perennial shrub. The basic information of *C. korshinskii* stand is given in Table 1. We hypothesized that soil properties for 1 depth is uniformity. This work was conducted based on Forestry Standards "Observation Methodology for Long–term Forest Ecosystem Research" of People′s Republic of China (LY/T 1952-2011).

**Table 1. Average soil properties for the top 1 m in Anjiapo catchment.**

| | | |
|---|---|---|
| Geographical attribution | Slope (°) | 15 |
| | Aspect (°) | 125 |
| Biological characteristics | Height (cm) | 170 |
| | Basic diameter (cm) | 1.51 |
| | Crown diameter (cm) | 115 |
| | Leaf area index (*LAI*) | 2.16 |
| | Age (year) | 26 |
| Soil properties | Clay (< 0.002 mm; %) | 9.17 |
| | Silt (0.05–0.002 mm; %) | 75.59 |
| | Sand (0.05–2 mm; %) | 15.24 |
| | Organic matter (%) | 0.68 |
| | PH | 8.1 |

*Slope, Aspect were measured by compass; *LAI* was determined by canopy analyzer (*LAI*–2000, LI–COR, USA); Soil organic matter was obtained by Potassium dichromate volumetric method; pH was determined by potentiometry; Soil texture was measured by sedimentation.

## Data collection

**Soil sampling:** Crown size of *C. korshinskii* was investigated in the study area. Four shrubs were selected with size approximate to the mean crown size with a distance to neighbouring trees of more than 10 m. The design of sampling position is shown in Fig. 1. The radius of sample area is 300 cm.

12 fiber tubes with 120 cm length were installed in the sampling section of each shrub to measure soil moisture (Fig. 1), which was measured at 10 cm intervals in each tube and at 7–day intervals from June to October in 2012 using a TDR (Campbell, CS–610).

The fine root length density (*FRLD*) was from soil cores, which were collected using a hand auger (6.5 cm internal diameter, 10 cm height) along three directions with the interval 20 cm in October of 2012. Soil samples were collected continuously in each point with 10 cm intervals to 120 cm depth (Fig. 1). Totally, 2160 soil samples were obtained. Samples were put into1 mm sieves and washed with a Gillion root elutriator. After washing, the dead and living roots were separated. The roots with diameter < 2 mm from living roots were picked out. The living fine roots in each layer were digitally scanned using a flatted scanner set at 600 dpi and saved as TIF files. Root images were analyzed using image analysis software (WinR–HIZO Pro 2008a, Regent Instruments Inc., Quebec City, Quebec, Canada) for root length. The fine root length density (*FRLD*, cm cm$^{-3}$) was calculated as follows: $FRLD = L/V_s$, where, $L$ is fine root length in each soil block, and $V_s$ is the volume of soil. Kriging interpolation method was used to analyze the fine roots two–dimensional distribution, and vertical profiles were divided into 10×20 cm grid cells based on the root sampling rules.

A soil profile was excavated in the study area near the sampled individuals to measure the soil hydraulic parameters, including soil water diffusivity ($D(\theta)$), unsaturated soil hydraulic conductivity($K(\theta)$), and suction curve. Two kinds of soil samples were collected. One was collected with standard core steel samplers (65 mm internal diameter and 50 mm height) with 10 cm intervals in the soil profile to obtain the suction curve which consists of soil water potential and soil water content. The soil water potential was measured by centrifuge method, soil water content corresponding to a certain soil water potential was obtained by conventional oven method. The suction curve obtained by fitting soil water content and soil water potential. The other one was taken in different layer of the soil profile and kept separately in plastic bags. These samples were air dried at room temperature for one week and sieved through a 1 mm sieve. Then the air dried soil samples were put into horizontal soil column and measured soil water diffusivity ($D(\theta)$). Soil hydraulic conductivity ($K(\theta)$) was calculated as follows:

$$K(\theta) = C(\theta)D(\theta) \qquad (1)$$

where, $C(\theta)$ is specific water capacity, which is reciprocal of the slop of the suction curve and expressed as:

$$C(\theta) = -\frac{d\theta}{dh} \qquad (2)$$

where, $h$ is the soil water potential (MPa), $\theta$ is the soil water content (cm$^3$ cm$^{-3}$).

**Plant transpiration:** Stem flow gauges were used (Flow4, Dynamax Inc., Houston, TX, USA) to measure sap flow of *C. korshinskii*. The theoretical method and methodology of sap flow gauge have been described by Smith & Allen (1996) and Yue *et al*. (2006). A total of 8 stems, out of the 4 sampled *C. korshinskii* individuals, were selected based on a statistical analysis within the study area for determining the mean stem. The selected stems were in good condition and well developed to support the weight of the sensor and survive throughout the measurement period. First stems were smoothed to remove any superficial bark roughness using a razor blade and put a layer of G4 silicon grease to basal stems at least 40 cm above the soil surface, then attaching gauges on the layer. The gauges were wrapped in aluminum foil to shield them from rain and direct solar radiation and reduce thermal energy transformation. The data were recorded at 10–s intervals and stored as 30–min averages.

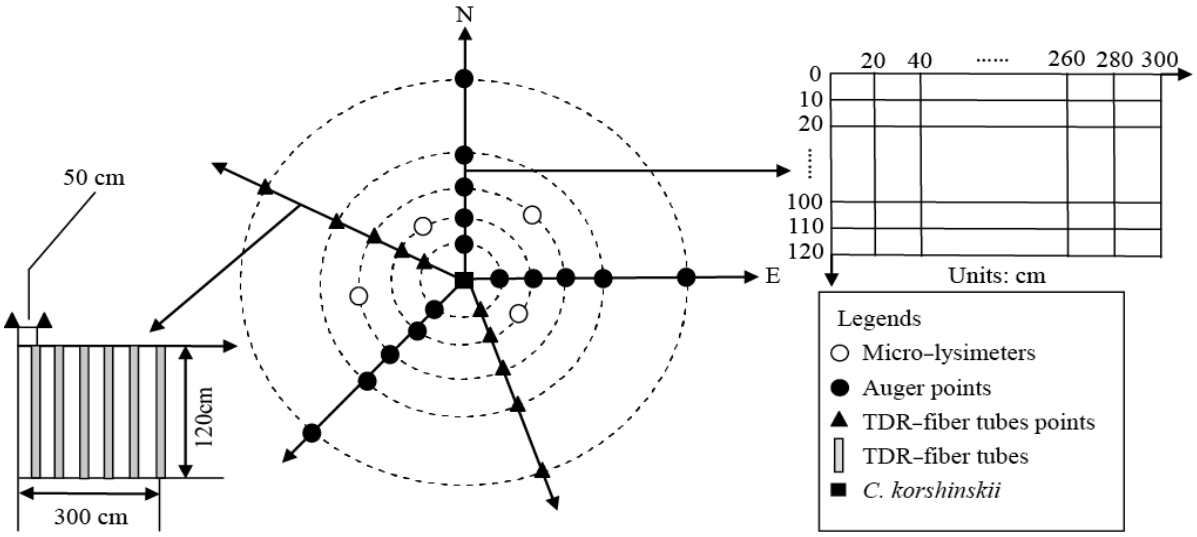


Fig. 1. The sketch map of root sampling.

**Soil evaporation:** Soil evaporation was measured with micro–lysimeters (Hopmans & Guttièrez–Ravé, 1982). Four micro–lysimeters were installed near the sample shrubs. They had an internal diameter of 25 cm and a height of 30 cm. The bottom of each micro–lysimeter was connected with a steel box that collected the drainage of water. The measurements were conducted at 09:00 and 17:00 in each day during the experimental period.

## Model description

**Root water uptake model:** The revised Feddes model was selected based on Feddes model (Feddes, 1978). The revised model is introduced by the water potential parameter as an additional item and expressed as:

$$S(r,z,t)=\frac{\pi R^2\alpha(h)L(r,z)}{2\pi\iint_D \alpha(h)L(r,z)rdrdz}T_r(t) \quad (3)$$

where $S(z, r, t)$ water uptake intensity (cm day$^{-1}$), $L(z, r)$ is two–dimension distribution of *FRD* (cm cm$^{-3}$), $z$ is soil depth (cm), $r$ is horizontal distance (cm), $R$ is maximum sampling length (300 cm), $D$ is domain of integration ($0 \le z \le 120$ cm; $0 \le r \le 300$ cm), $T_r(t)$ is the plant transpiration (cm day$^{-1}$), $\alpha(h)$ is the water potential function which is given as:

$$\alpha(h)=\begin{cases}\dfrac{h}{h_1} & h_1 \le h \le 0\\ 1 & h_2 \le h \le h_1\\ \dfrac{h-h_3}{h_2-h_3} & h_3 \le h \le h_2\\ 0 & h \le h_3\end{cases} \quad (4)$$

where $h$ is the water potential, $h_1$、$h_2$、$h_3$ are the threshold value of water potential of root water uptake. $h_1$ is the water potential when soil water content equals 80% field capacity, $h_2$ is the water potential when soil water content equals 60% field capacity, $h_3$ is the water potential when soil water content equals wilting moisture.

**Soil water movement equation in the root zone:** Soil water content in the root zone was simulated using the following equation, which is based on the Richards' equation (Lei *et al*., 1984). The equation is presented as:

$$\frac{\partial\theta}{\partial t}=\frac{1}{r}\frac{\partial}{\partial r}\left[rD(\theta)\frac{\partial\theta}{\partial r}\right]+\frac{\partial}{\partial z}\left[D(\theta)\frac{\partial\theta}{\partial z}\right]-\frac{\partial K(\theta)}{\partial z}-S(r,z,t)$$

$$\theta(r,z,0)=\theta_0(r,z), 0\le z\le z_m, 0\le r\le r_m$$

$$D(\theta)\frac{\partial\theta}{\partial z}+K(\theta)\Big|_{z=0}=-E_t(t)$$

$$\frac{\partial\theta}{\partial r}=0, when \quad r=0 \quad or \quad r=r_m$$

$$D(\theta)\frac{\partial\theta}{\partial z}+K(\theta)\Big|_{z=z_m}=-E_t(t) \quad (5)$$

where $E_t(t)$ is soil evaporation rate (cm day$^{-1}$), $z_m$ = 120 cm, $r_m$ = 300 cm, other symbols have the same meanings as Eq. (1), Eq. (2) and Eq. (3). The soil moisture was calculated using alternating implicit difference scheme based on Eq. (5). The spatial step: $\Delta z$ is 10 cm, $\Delta r$ is 20 cm. The time step ($\Delta t$) is 1day.

## Results

**Soil hydraulic parameters:** Table 2 showed the soil hydraulic parameters of *C. korshinskii* stand in the Anjiapo catchment, which is used to simulate soil moisture dynamic.

**The distribution of the *FRLD*:** The *FRLD* decreased significantly ($p$<0.05) with increasing soil depth (Fig. 2A). Fine roots were concentrated in the top of 80 cm, where the fine root length accounted for 91.18% of that in whole soil profile. The maximum *FRLD* density appeared at the soil layer of 30–40 cm. The regression equation between *FRLD* ($L(z)$) and soil depth ($z$) is expressed as:

$$L(z) = 1.149\, e^{-2.65z},\ R^2 = 0.721 \quad (6)$$

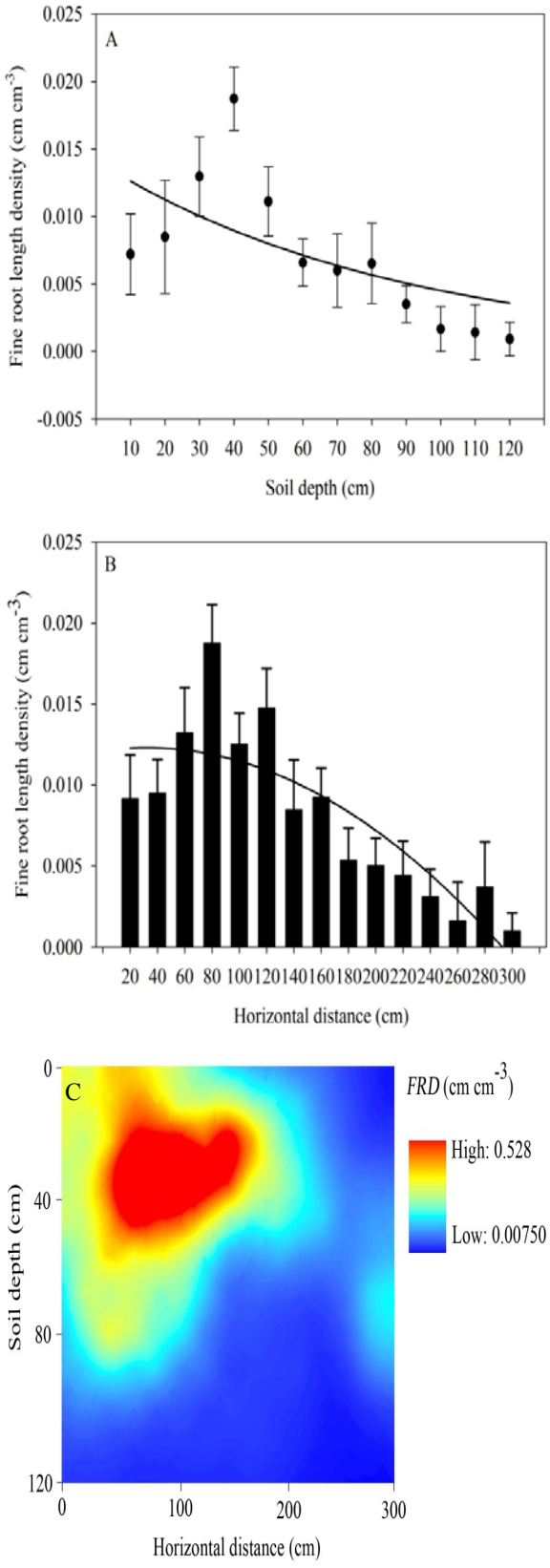


Fig. 2. Variation of *C. korshinskii FRLD* (A: the vertical variation (mean ± SD); B: the horizontal variation (mean ± SD); C: two–dimensional variation).

**Table 2. Soil hydraulic parameters in the Anjiapo catchment on the Loess Plateau, China.**

| **Soil hydraulic parameter** | |
|---|---|
| Suction curve | $h = 4.04\theta^{-1.36}$ |
| Soil water diffusivity | $D(\theta) = 7.75\theta^{4.98}$ |
| specific water capacity | $C(\theta) = 0.036\theta^{2.41}$ |
| unsaturated soil hydraulic conductivity | $K(\theta) = 0.28\theta^{7.39}$ |
| Soil water potential (Mpa) | |
| At field capacity (25.5%) | -0.491 |
| At 80% field capacity | -0.066 |
| At 60% field capacity | -0.984 |
| At wilting moisture (3.8%) | -1.5 |

The *FRLD* increased significantly ($p$<0.05) with increasing horizontal distance, and reached the maximum at 80 cm, and then decreased with increase of the distance (Fig. 2B). Fine roots mainly concentrated the section from 60 to 120 cm, where the fine root length accounted for 50.01% of that in whole section. The regression equation between *FRLD* ($L(r)$) and the horizontal distance ($r$) is:

$$L(r) = -7.24E\text{-}05\ r^2 + 2.34E\text{-}04r + 0.021,\ R^2 = 0.802 \quad (7)$$

The Kriged map of *FRLD* showed two dimensional distribution of *FRLD*. The fine roots concentrated in the upper soil layers ($20 < z < 50$ cm, $60 < r < 120$ cm). *FRLD* varied more rapidly in the vertical direction than the horizontal direction from the map (Fig. 2C). The regression equation between ($L(z, r)$) and soil depth ($z$) and horizontal distance ($r$) is expressed as:

$$L(z,r) = 0.791e^{-0.5[(\frac{z-3.891}{0.959})^2+(\frac{r-1.029}{0.514})^2]},\ R^2 = 0.704 \quad (8)$$

**The relationship between soil moisture and the distribution of *FRLD*:** There was a significantly negative correlation between the soil moisture and *FRLD* ($R^2$ = -0.65, $p$<0.001). The upper soil layers (0–20 cm) had the relative lower soil moisture and lower *FRLD*. That implied the lost water mainly resulted from evaporation. The soil layers (20–40 cm) had the lowest soil moisture and the highest *FRLD*. The result showed the lost water mainly resulted from root water uptake. Soil water content was approximate to wilting moisture (3.8%). Soil moisture increased with decreasing *FRLD* in the soil layers (40–90 cm). Below 90 cm, soil moisture kept stable because of few fine roots and no soil evaporation (Fig. 3).

**Plant transpiration:** Fig. 4 showed the diurnal variation of *C. korshinskii* transpiration from 1st June to 18th September in 2012. During the observed period, the transpiration was lowest at the beginning, increased with the time and reached the higher values (0.23 cm day$^{-1}$) in the middle ten days of August (from 224 to 233 Julian days), and then decreased with time till the end of the period. According to statistics of monthly transpiration, the ranking was June (0.074 cm day$^{-1}$) < September (0.11 cm day$^{-1}$) < July (0.12 cm day$^{-1}$) < August (0.21 cm day$^{-1}$).

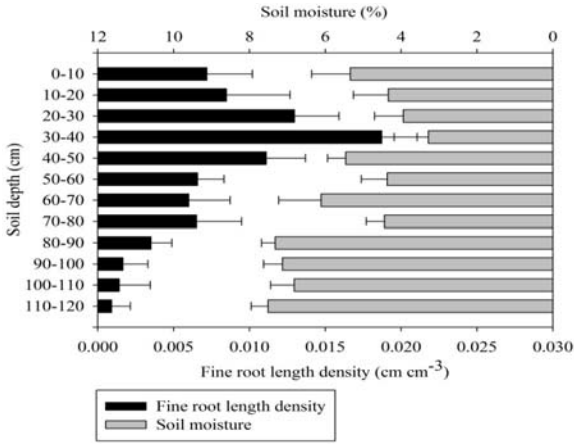


Fig. 3. Relationship between soil moisture and the distribution of *C.korshinskii FRLD*.

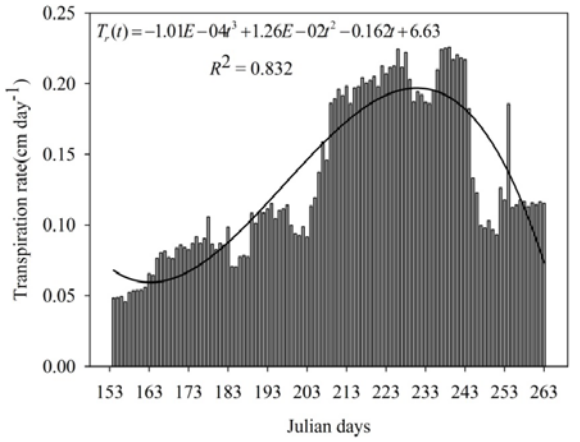


Fig. 4. Diurnal variation of *C. korshinskii* transpiration rate.

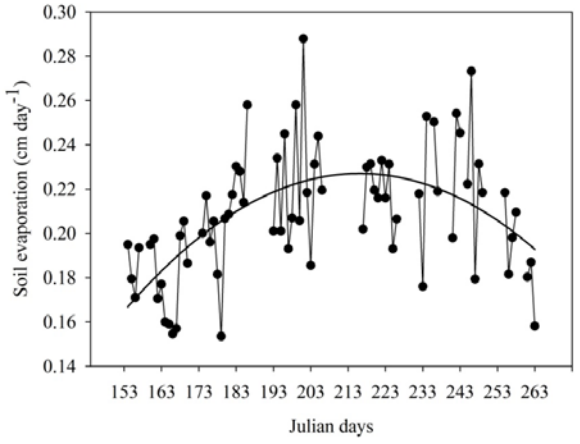


Fig. 5. Diurnal variation of soil evaporation.

**Soil evaporation:** Fig. 5 showed the trend of soil evaporation variations with time. During the experimental period, the soil evaporation increased with the time and reached the higher values (0.28 cm day$^{-1}$) in the beginning ten days of August (from 214 to 224 Julian days), and then decreased with time till the end of the period. Evaporation values varied from 0.15 to 0.29 cm per day. The ranking of monthly soil evaporation was June (0.18 cm day$^{-1}$) < September (0.20 cm day$^{-1}$) < July (0.22 cm day$^{-1}$) < August (0.23 cm day$^{-1}$).

**Root water uptake model**

**The model construction:** Based on the Eq. (3) and Eq. (4), root water uptake model of *C. korshinskii* was constructed. The formula is as follow:

$$S(z,r,t) = \begin{cases} a_1\alpha(h)_1 L(z,r)Tr(t) & 0 < z \le 10 \\ a_2\alpha(h)_2 L(z,r)Tr(t) & 10 < z \le 20 \\ a_3\alpha(h)_3 L(z,r)Tr(t) & 20 < z \le 30 \\ a_4\alpha(h)_4 L(z,r)Tr(t) & 30 < z \le 40 \\ a_5\alpha(h)_5 L(z,r)Tr(t) & 40 < z \le 50 \\ a_6\alpha(h)_6 L(z,r)Tr(t) & 50 < z \le 60 \\ a_7\alpha(h)_7 L(z,r)Tr(t) & 60 < z \le 70 \\ a_8\alpha(h)_8 L(z,r)Tr(t) & 70 < z \le 80 \\ a_9\alpha(h)_9 L(z,r)Tr(t) & 80 < z \le 90 \\ a_{10}\alpha(h)_{10} L(z,r)Tr(t) & 90 < z \le 100 \\ a_{11}\alpha(h)_{11} L(z,r)Tr(t) & 100 < z \le 110 \\ a_{12}\alpha(h)_{12} L(z,r)Tr(t) & 110 < z \le 120 \end{cases} \quad (9)$$

where $Tr(t)$ is measured by the stem–heat balance method, $L(z,r)$ is determined by Eq. (8), $\alpha(h)_1$–$\alpha(h)_{12}$ are calculated by Eq. (4) according to observed soil water content at a certain time. $a_1$–$a_{12}$ are the computational constants by Eq. (3). During the experimental period, the observed data of soil water content account to 16 times, therefore there are 16 pairs $a_n\alpha(h)_n$ in each soil layer (Table 3).

**Soil moisture simulation:** Soil moisture was simulated based on Eq. (5). The distribution of soil moisture of each day in the experiment period was obtained. The distribution maps of simulated soil moisture on two representative days were displayed (22$^{nd}$ June, no rainfall lasted for 14 days before the day; and 14$^{th}$ July, the rainfall occurred the day before) (Fig. 6). Fig. 6A depicted simulated soil water content distribution after continuous sunny days. The low soil water content centered at depth 20–50 cm and radial distance 0–180 cm. Fig. 6B depicted simulated soil water content distribution after rainy day, the surface soil water content approximate to 20%, and the soil water content beneath the canopy (0–110 cm) is lower than the soil water content beyond the canopy (180–300 cm), this may be the effects of canopy interception. The area around the stem, the higher soil water content extended to deeper soil layer (100 cm), this may be the effects of stemflow. Table 4 showed the relative errors and $R^2$ between simulated soil water content and observed values.

The results showed that the relative error varied from 9.59% to 18.57%, averaged 13.48%. The observed values agreed closely with the simulated values excellent.

**Table 3. The computational constants in the Eq. (9).**

| Observed time | $a_1\alpha(h)_1$ | $a_2\alpha(h)_2$ | $a_3\alpha(h)_3$ | $a_4\alpha(h)_4$ | $a_5\alpha(h)_5$ | $a_6\alpha(h)_6$ | $a_7\alpha(h)_7$ | $a_8\alpha(h)_8$ | $a_9\alpha(h)_9$ | $a_{10}\alpha(h)_{10}$ | $a_{11}\alpha(h)_{11}$ | $a_{12}\alpha(h)_{12}$ |
|---|---|---|---|---|---|---|---|---|---|---|---|---|
| June 2nd | 0.92 | 0.85 | 0.75 | 1.01 | 1.15 | 1.24 | 1.54 | 0.98 | 0.48 | 0.84 | 0.67 | 0.42 |
| 9th | 0.71 | 0.57 | 0.35 | 0.85 | 0.37 | 0.52 | 0.63 | 0.54 | 1.04 | 1.05 | 1.25 | 0.91 |
| 16th | 0.42 | 0.34 | 0.31 | 0.58 | 0.42 | 0.35 | 0.24 | 0.58 | 0.67 | 0.42 | 0.34 | 0.34 |
| 22nd | 1.57 | 1.48 | 1.48 | 1.10 | 1.36 | 0.94 | 0.87 | 0.68 | 1.10 | 1.025 | 1.17 | 1.04 |
| 30th | 1.84 | 1.75 | 1.47 | 1.68 | 1.71 | 1.67 | 1.54 | 1.25 | 0.97 | 0.98 | 1.24 | 0.99 |
| July 7th | 1.98 | 1.75 | 1.68 | 2.01 | 2.24 | 2.01 | 1.01 | 1.25 | 0.95 | 0.74 | 0.68 | 0.71 |
| 14th | 2.74 | 1.91 | 1.84 | 2.72 | 2.00 | 1.45 | 1.32 | 1.47 | 2.11 | 2.07 | 2.18 | 1.91 |
| 21st | 1.14 | 1.27 | 1.48 | 1.94 | 0.96 | 0.71 | 1.24 | 1.42 | 0.94 | 0.97 | 1.48 | 1.25 |
| 30th | 2.47 | 2.14 | 1.98 | 2.14 | 1.94 | 1.87 | 1.68 | 1.57 | 1.85 | 1.46 | 1.37 | 1.21 |
| Aug. 7th | 2.01 | 1.98 | 2.24 | 2.13 | 2.11 | 1.97 | 1.57 | 1.68 | 1.58 | 1.46 | 1.34 | 1.31 |
| 14th | 3.56 | 3.14 | 3.01 | 3.64 | 3.57 | 2.14 | 2.11 | 2.21 | 2.34 | 2.15 | 2.74 | 2.01 |
| 19th | 3.25 | 3.07 | 2.95 | 3.45 | 3.01 | 2.94 | 2.87 | 2.64 | 1.57 | 2.14 | 2.63 | 1.14 |
| 27th | 3.31 | 3.14 | 2.47 | 3.04 | 2.47 | 2.68 | 2.58 | 2.49 | 2.67 | 2.38 | 2.01 | 1.87 |
| Sept. 2nd | 2.45 | 2.38 | 2.18 | 1.92 | 1.34 | 1.21 | 1.57 | 1.41 | 1.13 | 0.97 | 0.84 | 0.61 |
| 9th | 1.85 | 1.68 | 1.54 | 2.01 | 1.58 | 1.42 | 1.36 | 1.24 | 1.15 | 1.35 | 1.04 | 0.94 |
| 17th | 1.14 | 1.24 | 1.03 | 1.45 | 1.55 | 1.24 | 1.13 | 1.08 | 1.14 | 1.24 | 0.95 | 0.74 |

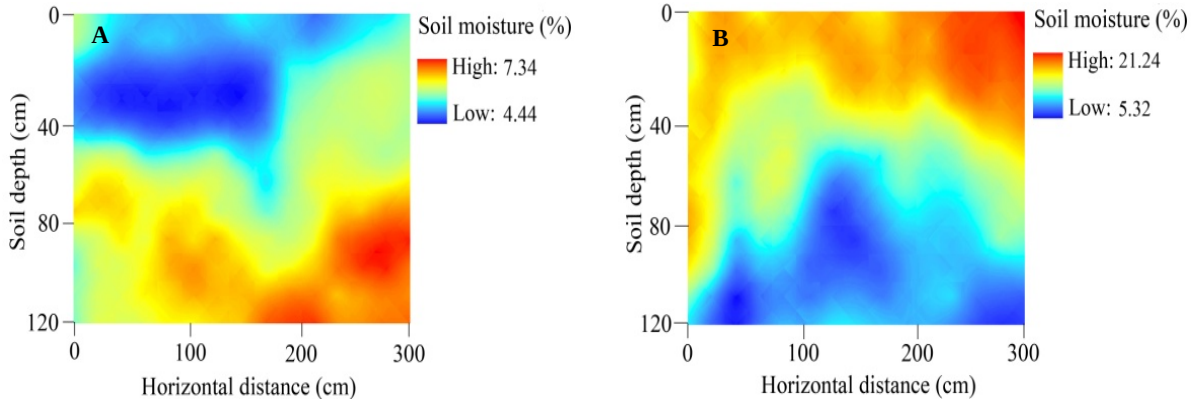


Fig. 6. The soil water content simulated results in the two presented days. A: 22nd June; B:14th July.

**Table 4. Simulated results of the model.**

| Time | Averaged relative error % | Max relative error % | $R^2$ |
|---|---|---|---|
| June. 2nd | 16.21 | 29.84 | 0.607 |
| 9th | 17.40 | 41.21 | 0.664 |
| 16th | 12.06 | 35.46 | 0.587 |
| 22nd | 15.14 | 40.89 | 0.712 |
| 30th | 12.72 | 28.94 | 0.745 |
| July 7th | 12.45 | 39.87 | 0.683 |
| 14th | 14.15 | 31.58 | 0.733 |
| 21st | 12.37 | 35.42 | 0.578 |
| 30th | 16.07 | 36.15 | 0.601 |
| Aug. 7th | 10.11 | 38.08 | 0.654 |
| 14th | 9.75 | 41.21 | 0.704 |
| 19th | 11.42 | 25.77 | 0.645 |
| 27th | 9.59 | 37.42 | 0.778 |
| Sept. 2nd | 14.25 | 21.26 | 0.621 |
| 9th | 18.57 | 28.14 | 0.694 |
| 17th | 13.40 | 28.03 | 0.751 |

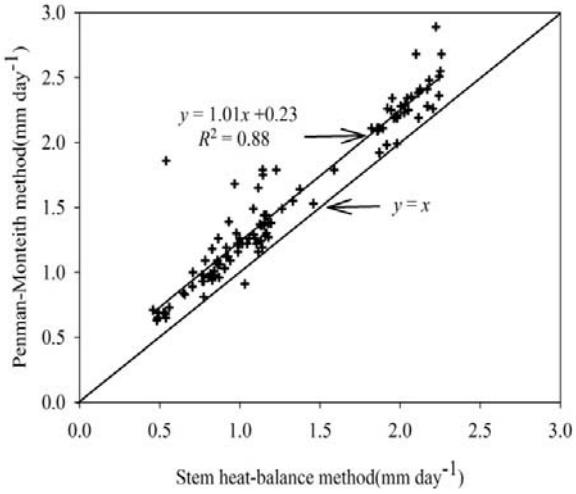


Fig. 7. The comparison of Penman–Monteith method and stem–heat balance method.

## Discussion

Our objectives were to describe fine–root systems distribution of *C. korshinskii* in the Anjiapo catchment, Loess Plateau, China. The relationship between fine roots and soil moisture was determined. Further, the root water uptake model of *C. korshinskii* was constructed, and simulated soil moisture dynamic in *C. korshinskii* woodland.

**The *FRLD* distribution:** Consistent with previous studies in most ecosystems, fine root density decreased exponentially with soil depth (Cairns *et al*., 1997; Jobbágy & Jackson, 2000). Our results are similar to the above studies. On average, estimated total fine root density in the top 50 cm depth, which accounted for 74.24% was higher than 63% expected for temperate deciduous vegetation (Jackson *et al*., 1996). Such a shallow fine root distribution in the current study, especially in the top 40 cm improves root water uptake in water–limited environments, where rainfall occurs as scarce shallow pulses. However during prolonged dry periods, plants may encounter severe water stress. The relationship between soil depth and *FRLD* also can be modeled by the equation (Gale & Grigal, 1987)

$$Y = 1 - \beta^z \quad (10)$$

where $z$ is depth (cm), $Y$ is the proportion of roots from the surface to depth $z$ and $\beta$ is a numerical index of rooting distribution. High values of $\beta$ indicate greater proportion of roots with depth (Jackson *et al*., 1996). The vegetation in the current study region ($\beta$ = 0.943) can be regarded as most similar to other deciduous vegetation such as temperate deciduous woodland ($\beta$ = 0.966) or sclerophyllous shrub land ($\beta$ = 0.964). Comparison with other forest ecosystems based on the Jackson *et al*. (1996) model showed that the computed root extinction coefficient ($\beta$) value was lower than that expected for sclerophyllous, temperate deciduous woodlands. The root extinction coefficient and the depth distribution of cumulative fine roots length in for the current study site obviously indicated a shallow fine root distribution, resembling that of grasslands and boreal forests ($\beta$=0.947) (Jackson *et al*., 1996).

Lateral extent of woody roots may exhibit a high degree of plasticity and depend on environmental conditions. Belsky (1994) found that *Acacia tortillis* trees from a dry site had lateral roots extending well beyond the canopy, but that trees from a wetter site concentrated their root growth beneath the canopy. She speculated that in more arid conditions *A. tortillis* invested in laterally extensive roots for greater water access, and when water was less limiting, *A. tortillis* roots grew under the canopy where nutrients were more plentiful. Our results are similar to this study, the distance of root lateral extent is about 1.5 times of crown size.

The distribution of fine roots implies that in the presence of soil moisture, root water uptake and probably deep drainage will show considerable patchiness consistent with radial distribution of fine roots. At stand scale, it has been reported that high spatial variability and clustered fine root systems reduce root water uptake compared to uniformly distributed root systems (Long *et al*., 2012). While root length vertical distribution is an important factor in most soil–plant–atmosphere models (Steingrobe *et al*., 2001), the distribution of fine roots may need to be accounted for in models for systems like the one studied in our site. Using root data based on a few samples may entail substantial uncertainties in result of water balance simulations for certain vegetation ecosystem.

**Soil moisture and *FRLD* distribution:** Soil moisture decreased with increasing *FRLD* for single individual in each soil layer (Fig. 5). In our study site, little rain, strong surface evaporation, resulting in soil moisture dramatic change of soil layer 0–50 cm. The relationships between roots and water uptake were discussed in several reports (Robertson & Fukai, 1994; Dardanelli *et al*., 2004). A general conclusion was that deeper rooted plants were more likely to tolerate durable periods of drought by accessing more moist soil layers (Chaves *et al*., 2002; Du *et al*., 2014). Nonetheless, whether root size is significantly related to water uptake is still uncertain as there is not unequivocal evidence that this relationship is always true. Some authors reported the positive relations between root development and water uptake (Amato & Ritchie, 2002), while others demonstrated that the ability of the plant in recovering water could be independent from the root size (Steingrobe *et al*., 2000; Vamerali *et al*., 2003).

The soil evaporation and fine roots water uptake deplete the moisture of soil layers, and the soil might be divided into two regions: the wet layer and the dry layer (Bogeat–Triboulot *et al*., 2007). In the current paper, the relative soil dry layer is 30–40 cm, fine roots water uptake plays a key role, because the soil evaporation has little influence on the soil layer (Chen *et al*., 2007). As an unsaturated porousmedium, the wet soil consists of solid particles, liquid water, gaseous mixture of vapor and air and other chemical and biological substances. Heat and moisture transfers in the wet region are highly coupled. However, there is no free water in a dry layer and soil is saturated with gas (Hardtke & Torii, 2008). Dry soil layer has a significant effect on heat and mass transfer in soil. With the development of dry soil layer, evaporation front moves from the upper soil surface to the interface between the wet and dry layers, while soil temperature increases remarkably and water evaporation rate reduces significantly due to the increase of vapor diffusion resistance to atmosphere (Chen *et al*., 2007; Zhao *et al*., 2014).

**Soil moisture simulation:** Soil water content verification test results suggested that the simulated soil water content reflected the actual condition of *C. korshinskii* root water uptake. Under the influence of specific environment, the simulated process had some limitations inevitably, due to all the parameters in the model were fitting based on measured data. The simulation of soil water content had high reliability in specific location (Loess Plateau of Northwest China) and specific time (the growth season), specific species (*C. korshinskii*).

The simulated results were determined by three parameters: *FRLD* function ($L$), water potential function ($\alpha(h)$) and plant transpiration rate ($T_r(t)$). The fitting precision of three parameters had a direct influence on the simulated precision, to improve simulated precision from the three aspects. In literatures, some scholars set up the water potential function ($\alpha(h)$) based on the average of soil moisture, which makes $\alpha(h)$ a defined piecewise function (Feddes, 1976; Li & Huang, 2008), and thus affects the accuracy of simulation results. In this paper, the corresponding $\alpha(h)$ was drawn according to the specific soil condition, and made the simulated results more reasonable. It is difficult to improve *FRLD* function ($L$). The fitting accuracy should be improved by the choice of appropriate fitting function. To improve the transpiration rate ($T_r(t)$), Penman–Monteith equation can be used to revise the transpiration rate (Fig. 7).

## Conclusion

The aim of this study was to understand better and effectively the dynamics of the root water uptake by the single *C. korshinskii* individual in relation to spatial and temporal distribution of soil water and fine roots. The models for single *C. korshinskii* individual were verified with soil moisture in *korshinskii* woodland. Oven–dry method was used to measure soil moisture, and sap flow sensors based on stem–heat technology were used to monitor locally the rates of sap flow in the trunk of *C. korshinskii*. Soil water potential function was determined by the suction curve. Root density distribution was determined for the purpose of simulated soil water movement in the root zone under *C. korshinskii*, and made certain the relationships between fine roots distribution and soil moisture. In general, there was a very good agreement between the measured and the simulated results. The models can be used in the uneven root distribution in the vertical and radical directions in the root zone of *C. korshinskii*. The root water uptake models have considered the spatial variability of soil water and roots distribution to some extent, which almost reached the condition of field, so the measured and simulated results were almost similar.

## Acknowledgements

This paper was supported by Special Fund for Forestry Scientific Research in the Public Interest (No. 201204101–4), National Natural Science Foundation of China (No. 31260141). This paper was supported by CFERN & GENE Award Funds on Ecological Paper.

### References

Amato, M. and J.T. Ritchie. 2002. Spatial distribution of roots and water uptake of maize (*Zea mays* L.) as affected by soil structure. *Crop Sci*., 42: 773-780.

Belsky, A.J. 1994. Influences of trees on savanna productivity: tests of shade, nutrients and tree–grass competition. *Ecology*, 75: 922-932.

Bogeat–Triboulot, M.B., M. Brosche and J. Renaut. 2007. Gradual soil water depletion results in reversible changes of gene expression, protein profiles, ecophysiology, and growth performance in *Populus euphratica*, a poplar growing in arid regions. *Plant Physiol*., 143: 876-892.

Cairns, M.A., S. Brown, E.H. Helmer and G.A. Baumgardner. 1997. Root biomass allocation in the world's upland forest. *Oecologia*, 111: 1-11.

Chaves, M.M., J.S. Pereira, J. Maroco, M.L. Rodrigues, C.P.P. Ricardo, M. L. Osório, I. Carvalho, T. Faria and C. Pinheiro. 2002. How plants cope with water stress in the field? Photosynthesis and growth. *Ann. Bot*., 89: 907-916.

Chen, H.S., M.A. Shao and Y.Y. Li. 2008. Soil desiccation in the Loess Plateau of China. *Geoderma*, 143: 91-100.

Chen, L.D., W. Wei, B.J. Fu and Y.H. Lü. 2007. Soil and water conservation on the Loess Plateau in China: review and perspective. *Prog. Phys. Geog*., 31: 389-403.

Cheng, X. 2002. Relationship between agriculture and ecological deterioration, restoration and reconstruction in Loess Plateau areas of Northwest China. *Agr. Sci. China*, 1: 114-120.

Dardanelli, J.L., J.T. Ritchie, M. Calmon, J.M. Andiani and D.J. Collino. 2004. An empirical model for root water uptake. *Field Crop. Res*., 87: 59-71.

Donaldson, L.A. and M.J.F. Lausberg. 1998. Comparison of conventional transmitted light and confocal microscopy for measuring wood cell dimentions by image analysis. *IAWA J.*, 19: 321-336.

Du, B.M., H.Z. Kang, J. Pumpanen, P.H. Zhu, S.Y.Q. Zou, Z.W.F.Q. Kong and C.J. Liu. 2014. Soil organic carbon stock and chemical composition along an altitude gradient in the Lushan Mountain, subtropical China. *Ecol. Res*., 29: 433-439.

Feddes, R.A., P.J. Kowalik, K. Kolinska–Malinka and H. Zaradny. 1976. Simulation of field water uptake by plants using a soil water dependent root extraction function. *J. Hydrol*., 31: 13-26.

Feddes, R.A., P.J. Kowalik and H. Zaradny. 1978. Simulation of field water use and crop yield simulation monograph series. PUDOC, Wageningen.

Fromm, J., B. Rockel, E. Windeisen and G. Wanner. 2003. Lignin distribution in wood cell walls determined by TEM and backscattered SEM techniques. *J. Struct. Biol*., 143: 77-84.

Gale, M.R. and D.F. Grigal. 1987. Vertical root distributions of northern tree species in relation to successional status. *Can. J. Forest Res*., 17: 829-834.

Gardner, W.R. 1991. Modeling water uptake by roots. *Irrig. Sci*., 12: 109-114.

Green, S.R., I. Vogeler, B.E. Clothier, T.M. Mills and C. van den Dijssel. 2003. Modelling water uptake by a mature apple tree. *Aust. J. Soil Res*., 41: 365-380.

Hardtke, C. and K. Torii. 2008. Plant growth and development–the new wave. *Curr. Opin. Plant Biol*., 11: 1-3.

He, F.H., M.B. Huang and T.H. Dang. 2003. Distribution characteristic of dried soil layer in Wangdonggou watershed in gully region of the Loess Plateau. *J. Nat. Resour.*, 18: 30-36 (in Chinese with English abstract).

Hopmans, J.W. and E. Guttièrez–Ravé. 1988. Calibration of a root water uptake model in spatially variable soils. *J. Hydrol*., 103: 53-65.

Huang, M.B., J. Gallichand and L.P. Zhong. 2004. Water–yield relationships and optimal water management for winter wheat in the Loess Plateau of China. *Irrig. Sci*., 23: 47-54.

Jackson, R.B., J. Canadell, J.R. Ehleringer, H.A. Mooney, O.E. Sala and E.D. Schulze. 1996. A global analysis of root distribution for terrestrial biomes. *Oecologia*, 108: 389-411.

Jobbágy, E.G. and R.B. Jackson. 2000. The vertical distribution of soil organic carbon and its relation to climate and vegetation. *Ecol. Appl*., 10: 423-436.

Kimura, R., L. Bai, J. Fan, N. Takayama and O. Hinokidani. 2007. Evapo–transpiration estimation over the river basin of the Loess Plateau of China based on remote sensing. *J. Arid Environ*., 68: 53-65.

Lacombe, G., B. Cappelaere and C. Leduc. 2008. Hydrological impact of water and soil conservation works in the Merguellil catchment of central Tunisia. *J. Hydrol.*, 359: 210-224.

Lai, C.T. and G. Katul. 2000. The dynamic role of root–water uptake in coupling potential to actual transpiration. *Adv. Water Res*., 23: 427-439.

Lei, Z.D., S.X. Yang and S.C. Xie. 1984. *Soil Water Dynamics*. Tsinghua University Press, China (in Chinese).

Li, Y.S. 1983. The properties of water cycle in soil and their effect on water cycle for land in the Loess Plateau.*Acta Ecol. Sinica*, 3: 91-101 (in Chinese with English abstract).

Li, Y.S. 2001. Effects of forest on water circle on the Loess Plateau. *J. Nat. Resour.*, 16: 427–432 (in Chinese with English abstract).

Li, Y.S. and M.B. Huang. 2008. Pasture yield and soil water depletion of continuous growing alfalfa in the Loess Plateau of China. *Agr. Ecosyst. Environ.*, 124: 3-12.

Long, F., S.C. Li, H.L. Sun and C.J. Li. 2012. Influence of limited soil on the root distribution and anchorage of *Vitex negundo* L. *J. Mt. Sci.*, 9: 723-730.

Morgenschweis, G. 1984. Soil–water movement and balance in thick loess soils and its model simulation. *J. Hydrol.*, 67: 339-360.

Macinnis–Ng, C.M.O., S. Fuentes, A.P. O'Grady, A.R. Palmer, D. Taylor, R.J. Whitley, I. Yunusa, M.J.B. Zeppel and D. Eamus. 2010. Root biomass distribution and soil properties of an open woodland on a duplex soil. *Plant Soil*, 327: 377-388.

Meng, Q.M. 1997. *Soil and Water Conversation in Loess Plateau*. Huanghe Hydraulic Press, China. (in Chinese).

Millikin, C.S. and C.S. Bledsoe. 1999. Biomass and distribution of fine and coarse roots from blue oak (*Quercus douglasii*) trees in the northern Sierra Nevada foothills of California. *Plant Soil*, 214: 27-38.

Molz, F.I. 1981. Models of water transport in the soil–plant system. A review. *Water Resour. Res*., 17: 1245-1260.

Odhiambo, H.O., C.K. Ong, J. Wilson, J.D. Deans, J. Broadhead and C. Black. 1999. Tree–crop interactions for below–ground resources in drylands: root structure and function. *Ann. Arid Zone*, 38: 221-237.

Robertson, M.J. and S. Fukai. 1994. Comparison of water extraction models for grain sorghum under continuous soil drying. *Field Crop. Res*., 36: 145-160.

Schenk, H.J. and R.B. Jackson. 2002. The global biogeography of roots. *Ecol. Monogr*., 72: 311-328.

Schroth, G. 1995. Tree root characteristics as criteria for species selection and systems design in agroforestry. *Agrofor. Syst*., 30: 125-143.

Smith, D.M. and S.J. Allen. 1996. Measurement of sap flow in plant stems. *J. Exp. Bot.*, 47: 1833-1844.

Steingrobe, B., H. Schmid and N. Claassen. 2001. The use of the in–growth core method for measuring root production of arable crops–influence of soil conditions inside the in–growth core on root growth. *Eur. J. Agron*., 15: 143-151.

Valverde–Barrantes, O.J., J.W. Raich and A.E. Russell. 2007. Fine–root mass, growth and nitrogen content for six tropical tree species. *Plant Soil*, 290: 357-370.

Vamerali, T., M. Saccomani, S. Bona, G. Mosca, M. Guarise and A. Ganis. 2003. A comparison of root characteristics in relation to nutrient and water stress in two maize hybrids. *Plant Soil*, 255: 157-167.

Wang, L., Q.J. Wang, S.P. Wei, M.A. Shao and Y. Li. 2008. Soil desiccation for Loess soils on natural and regrown areas. *Forest Ecol. Manag*., 255: 2467-2477.

Xu, F., X.C. Zhong, R.C. Sun and Q. Lu. 2006. Anatomy, ultra structure and lignin distribution in cell wall of *Caragana Korshinskii*. *Ind. Crop. Prod*., 24: 186-193.

Yang, W.Z. and J.L. Tian. 2004. Essential exploration of soil aridization in Loess Plateau. *Acta Pedol. Sinica*, 41: 1-6 (in Chinese with English abstract).

Yue, G.Y., T.H. Zhang, H.L. Zhao, L. Niu, X.P. Liu and G. Huang. 2006. Characteristics of sap flow and transpiration of *Salix gordejevii* and *Caragana microphylla* in Horqin Sandy Land, northeast China. *Acta Ecol. Sinica*, 26: 3205-3213 (in Chinese with English abstract).

Zhao, F.Q, H.S, He, L.M. Dai and J. Yang. 2014. Effects of human disturbances on Korean pine coverage and age structure at a landscape scale in Northeast China. *Ecol. Eng*., 71: 375-379.

(Received for publication 14 December 2013)